

NMR Studies of the Paramagnetic Complex Fe(II)–Bleomycin<sup>†</sup>Teresa E. Lehmann,<sup>‡</sup> Li-June Ming,<sup>§</sup> Mark E. Rosen,<sup>‡</sup> and Lawrence Que, Jr.\*<sup>‡</sup>

Department of Chemistry and Center for Metals in Biocatalysis, University of Minnesota, Minneapolis, Minnesota 55455, and  
Department of Chemistry and Institute for Biomolecular Science, University of South Florida, Tampa, Florida 33620

Received November 4, 1996; Revised Manuscript Received December 17, 1996<sup>⊗</sup>

**ABSTRACT:** The coordination chemistry of the iron(II) complex of the antitumor drug bleomycin has been extensively investigated with a number of spectroscopic and chemical techniques. However, the actual structure of this complex is not established. In this report, we present NMR studies of the paramagnetic Fe(II)BLM and use one- and two-dimensional methods to assign the paramagnetically shifted features to particular protons. The data analysis points toward the primary and secondary amines of the  $\beta$ -aminoalanine fragment, the pyrimidine and imidazole rings, and the amide nitrogen of the  $\beta$ -hydroxyhistidine fragment as ligands to the metal center. Correlation of the  $T_1$  values with the metal–proton distances derived from the NMR-generated solution structure of HOO-Co(III)BLM [Wu, W., Vanderwall, D. E., Lui, S. M., Tang, X.-J., Turner, C. J., Kozarich, J. W., & Stubbe, J. (1996) *J. Am. Chem. Soc.* 118, 1268–1280] indicates that the two metallobleomycins share similar structures. The chemical shifts as well as the  $T_1$  values of the sugar protons indicate that these fragments are close but not bound to the metal in Fe(II)BLM.

The bleomycins (Figure 1) are a group of glycopeptide antibiotics synthesized by *Streptomyces verticillus* that are widely used for the treatment of various neoplastic diseases (Lazo & Sebti, 1989). Cleavage of DNA by bleomycins likely accounts for the antibiotic and antitumor activities of this drug (Cullinam et al., 1991; Hecht, 1986). Bleomycins bind a number of transition metal ions. While the Co(III), Mn(II), and Fe(II) derivatives have been found to be able to degrade DNA, only the Fe complex is postulated as the active species *in vivo* (Absalon et al., 1995a,b; McGall et al., 1992). The coordination chemistry of the biologically relevant Fe(II)BLM<sup>1</sup> has been intensively investigated through the use of various spectroscopic and chemical techniques (Stubbe & Kozarich, 1987; Dabrowiak, 1982); however, the precise structure of this complex has remained elusive so far.

To gain some insight into the structure and coordination chemistry of the Fe complex of BLM, other possibly isostructural metallobleomycins have been investigated. The initial model for the metal coordination environment of the metallobleomycins was derived from the X-ray structure of a Cu(II) complex of a biosynthetic precursor of BLM, Cu(II)•P-3A (Itaka et al., 1978), which is missing both the sugar residues and the bithiazole tail. The crystal structure of Cu(II)•P-3A shows that the primary and secondary amines of the ALA moiety, the pyrimidine and imidazole rings, and

the amide nitrogen in the HIST segment are ligated to the Cu(II) center. Some of the subsequent studies performed on other metallobleomycins such as Fe(II)BLM (Sugiura et al., 1980) and Co(III)BLM (Wu et al., 1996) have supported the metal coordination environment proposed for Cu(II)•P-3A. However, on the basis of studies of Fe(II)(CO)BLM, two alternative metal coordination schemes were proposed where the carbamoyl group in the M moiety replaced either the amide nitrogen in the HIST fragment (Oppenheimer et al., 1982) or the primary amine in the ALA segment (Akkerman et al., 1990). The various studies concur on the notion that the active metal center is likely to be five-coordinate with the sixth site available for O<sub>2</sub> binding. Three of the metal ligands are the secondary amine of ALA, the pyrimidine, and the imidazole (Stubbe & Kozarich, 1987; Dabrowiak, 1982), but there are three candidates for the remaining two ligands: the amide nitrogen of the HIST moiety, the primary amine in ALA, and the mannose carbamoyl nitrogen.

Herein, we report NMR studies performed on Fe(II)BLM using one- and two-dimensional techniques. <sup>1</sup>H-NMR spectroscopy has proved very useful for probing the metal environments of many paramagnetic metalloproteins via the isotropically shifted resonances arising from the nuclei in close proximity to the metal center (Bertini & Luchinat, 1986). Pillai and co-workers (1980) were the first to report the NMR spectrum of Fe(II)BLM showing paramagnetically shifted features in the 70 to –20 ppm range. They used saturation transfer (ST) methods to assign these signals. We have followed up on this study and taken advantage of the advances in NMR methodology and instrumentation since this work to complement the ST results. Paramagnetically shifted resonances out to 230 ppm have been observed, and two-dimensional experiments have been employed to strengthen the initial assignments. Furthermore, the  $T_1$  values for these protons have been used to estimate metal–proton distances and to determine whether Fe(II)BLM adopts a solution structure similar to that found for HOO-Co(III)BLM from solution NMR studies (Wu et al., 1996a,b).

<sup>†</sup> This work was supported by the National Institutes of Health (Grants GM-33162 and GM-51849).

\* To whom correspondence should be addressed.

<sup>‡</sup> University of Minnesota.

<sup>§</sup> University of South Florida.

<sup>⊗</sup> Abstract published in *Advance ACS Abstracts*, March 1, 1997.

<sup>1</sup> Abbreviations: BLM, bleomycin; ALA,  $\beta$ -aminoalanine bleomycin fragment; PYR, pyrimidinylpropionamide bleomycin fragment; HIST,  $\beta$ -hydroxyhistidine bleomycin fragment; VAL,  $\alpha$ -methylvalerate bleomycin fragment; THR, threonine bleomycin fragment; BITH, bithiazole bleomycin fragment; DIM,  $\gamma$ -aminopropyltrimethylsulfonium bleomycin fragment; M, mannose bleomycin fragment; G, glucose bleomycin fragment; COSY, homonuclear correlation spectroscopy; HMQC, <sup>1</sup>H-detected heteronuclear multiple-quantum coherence; NOE, nuclear Overhauser effect; NOESY, nuclear Overhauser spectroscopy; ST, saturation transfer; TOCSY, total correlation spectroscopy.

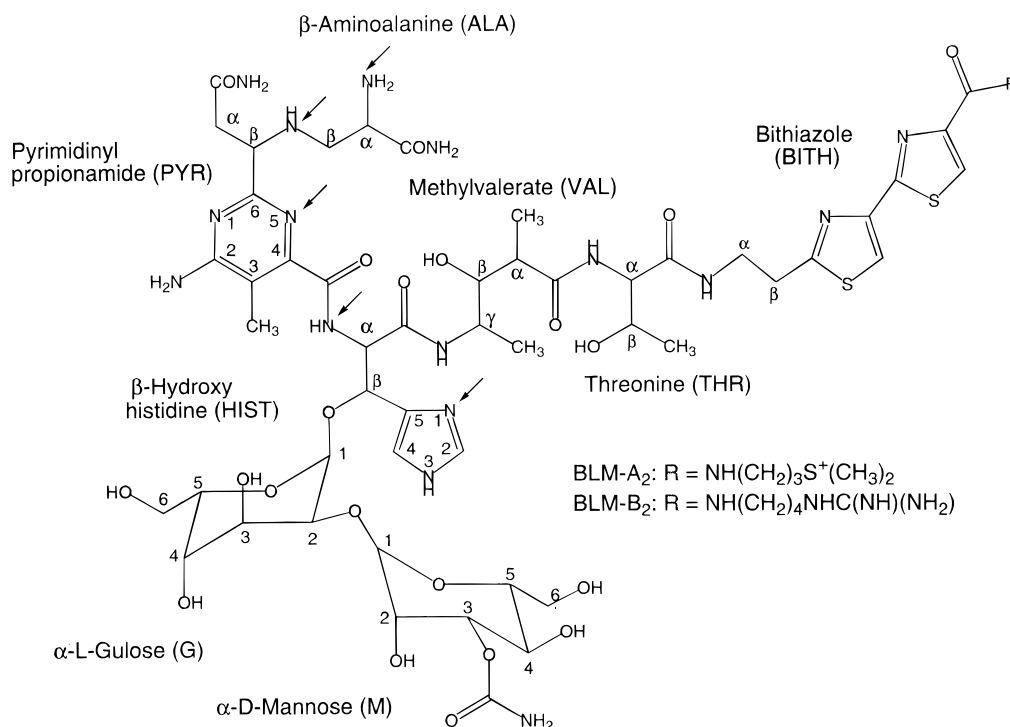


FIGURE 1: Structures of BLM-A<sub>2</sub> and BLM-B<sub>2</sub>, the most abundant components of the clinically employed mixture of bleomycins (Umezawa, 1973). The arrows indicate the ligands to the metal center proposed on the basis of the results of the present study.

## EXPERIMENTAL PROCEDURES

**Sample Preparation.** Bleomycin, the commercial mixture of bleomycin congeners, was a generous gift of A. J. Razel and S. J. Lucania, Bristol-Myers Squibb Pharmaceutical Research Institute (Princeton, NJ). The various bleomycins differ only with respect to the structure of the C-terminal amine (Figure 1). The commercial drug consists predominantly of a 3:1 mixture of BLM-A<sub>2</sub> and BLM-B<sub>2</sub> with trace quantities of other congeners. Most of the proton resonances are identical for BLM-A<sub>2</sub> and BLM-B<sub>2</sub>, and evidence from chemical shift studies suggests similar solution conformational characteristics for these two congeners (Chen et al., 1977). For these reasons, the commercial mixture was used in the experiments without further purification and is referred to as BLM. Due to the extreme sensitivity of Fe(II)BLM to oxidation, all samples were prepared under strict oxygen-free conditions. BLM (6  $\mu$ mol) lyophilized three times from D<sub>2</sub>O was dissolved in 0.6 mL of D<sub>2</sub>O (99.9% D, Cambridge Isotope Laboratories). This solution was divided into two parts of 300  $\mu$ L each. A solution of FeSO<sub>4</sub>·7H<sub>2</sub>O in D<sub>2</sub>O was added to both samples to afford BLM:Fe(II) ratios of 1:1 and 2:1. The pH (meter reading uncorrected for the deuterium isotope effect) was adjusted to 6.5 in each sample with a 50 mM NaOD solution. This was the optimum pH value to assure sufficient formation of the Fe(II)BLM complex without precipitation of the added Fe(II). Subsequently, 4.5  $\mu$ L of 20 mM sodium dithionite in D<sub>2</sub>O was added to each sample. The samples were transferred to purged NMR tubes, which were immediately sealed. A 1:1 BLM-Fe(II) sample in H<sub>2</sub>O was prepared by an analogous procedure.

**NMR Spectra.** NMR experiments were performed at 300, 360, and 500 MHz on Varian VXR300, Bruker AMX360, and Varian VXR500 NMR spectrometers. All chemical shifts were referenced to HDO as the internal standard. The solvent signal was selectively irradiated for 80 ms in all

spectra. The one-dimensional spectra were obtained using a 90° pulse (10–12  $\mu$ s on the Varian VXR500 and VXR300 spectrometers and 7  $\mu$ s on the Bruker AMX360 spectrometer) with 16K data points. An inversion–recovery pulse sequence (180°– $\tau$ –90°–AQ) was used to obtain nonselective proton longitudinal relaxation times ( $T_1$ ) with the carrier frequency set at several different positions to ensure the validity of the measurement. Signal:noise ratios were improved by applying a line-broadening factor of 30 Hz to the FID prior to Fourier transformation.

Saturation transfer experiments were performed on the 2:1 BLM-Fe(II) sample. The paramagnetically shifted signals were selectively saturated using gated homonuclear decoupling with a decoupling time of 0.08–1.0 s and decoupling power of 0.03 W. The ST response was determined from a difference spectrum obtained by subtracting the spectrum where the target signal is irradiated from a spectrum with the decoupler located at a neutral position.

Magnitude COSY spectra covering the 50 to –20 ppm region were collected on the VXR500 NMR spectrometer with 256 points in the  $t_2$  and  $t_1$  dimensions, a spectral width of 54 kHz, and a relaxation delay of 300 ms. COSY spectra covering the 0–15 ppm region were acquired with 2048 points in  $t_2$  and 512 points in  $t_1$ , a spectral width of 23 kHz, and a relaxation delay of 1 s when taken on the VXR500 NMR spectrometer. On the AMX360 spectrometer, 800 points in  $t_2$  and 400 points in  $t_1$  were acquired with a spectral width of 15 kHz and a repetition time of 300 ms. COSY spectra of Fe(II)BLM in H<sub>2</sub>O were also acquired on the AMX360 spectrometer in order to observe the correlations involving the exchangeable protons. For these spectra, 1024 points in  $t_2$  and 512 points in  $t_1$  were acquired with a spectral width of 39 kHz and a relaxation delay of 300 ms. A zero-degree-shifted sine bell was applied prior to Fourier transformation and followed by symmetrization in some spectra.

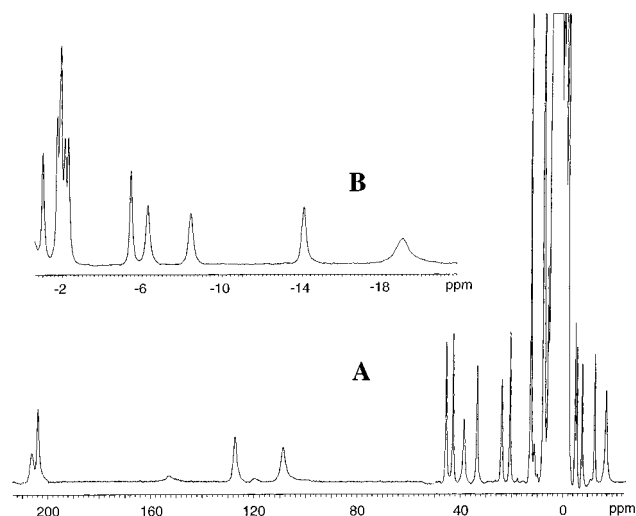


FIGURE 2: (A)  $^1\text{H-NMR}$  512-scan spectrum (Varian VXR300 instrument at 299.95 MHz and 298 K) of a 10 mM 1:1 BLM–Fe(II) sample in  $\text{D}_2\text{O}$ . (B) Region from  $-0.6$  to  $-21$  ppm of the  $^1\text{H-NMR}$  512-scan spectrum (Varian VXR300 instrument at 299.95 MHz and 288 K) of a 10 mM 1:1 BLM–Fe(II) sample in  $\text{D}_2\text{O}$  showing the upfield-shifted signals.

TOCSY spectra of Fe(II)BLM in both  $\text{D}_2\text{O}$  and  $\text{H}_2\text{O}$  were collected in order to identify some of the spin systems in Fe(II)BLM. Spectra of the  $\text{D}_2\text{O}$  sample were acquired on the AMX360 NMR spectrometer with 1024 points in  $t_2$  and 512 points in  $t_1$ , a spectral width of 31 kHz, a mixing time of 10 ms, and a relaxation delay of 100 ms. Spectra for the sample in  $\text{H}_2\text{O}$  were acquired with 800 points in  $t_2$ , 400 points in  $t_1$ , a spectral width of 20 kHz, a mixing time of 10 ms, and a relaxation delay of 100 ms. A  $60^\circ$ -shifted sine-squared bell was applied to both dimensions prior to Fourier transformation.

HMQC spectra were acquired on the VXR500 NMR spectrometer with 2048 points in  $t_2$  and 256 points in  $t_1$  and a spectral width of 6 kHz in the proton dimension and 30 kHz in the carbon dimension. A relaxation delay of 300 ms was used for the signals with  $T_1$ 's of  $>30$  ms and 20 ms for the signals with  $T_1$ 's of  $<30$  ms.

## RESULTS AND DISCUSSION

The one-dimensional  $^1\text{H-NMR}$  spectrum of Fe(II)BLM is shown in Figure 2A. It consists of well-resolved isotropically shifted resonances that span over 230 ppm, a chemical shift range significantly larger than originally reported by Pillai et al. (1980). The high resolution and the relatively narrow line widths observed in the spectrum are as expected for high-spin Fe(II) complexes (Bertini & Luchinat, 1986). Relative integration of the NMR signals indicates that they all arise from single protons with the exception of the resonances at 12.9 and 8.1 ppm which are derived from  $\text{CH}_3$  groups (vide infra). Because of overlap, the resonances positioned between  $-0.6$  and  $-3$  ppm in Figure 2B cannot be individually integrated but correspond to at least five protons when considered as a cluster. Most of the observed features have been assigned by a combination of approaches, including saturation transfer experiments to relate paramagnetically shifted features with their diamagnetic congeners, two-dimensional experiments (COSY, TOCSY, and HMQC) to establish scalar connectivity, and  $T_1$  measurements to determine proximity to the iron(II) center. We have used as a

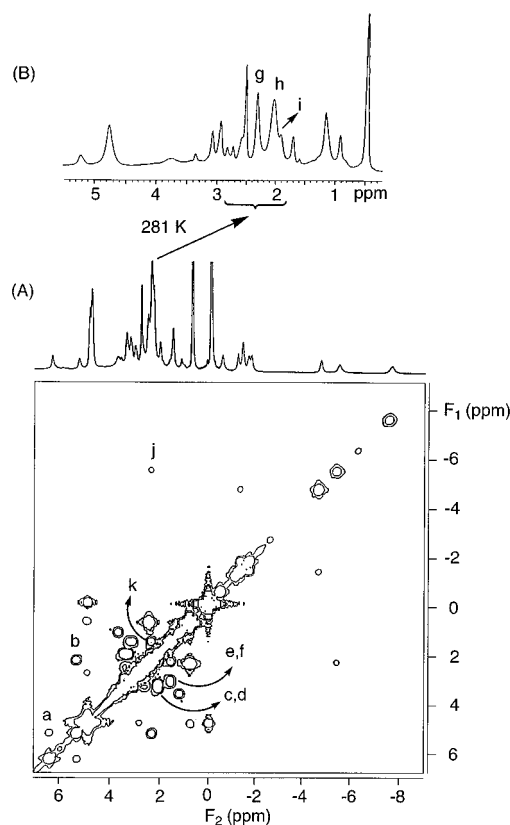


FIGURE 3: (A)  $^1\text{H-COSY}$  400-scan spectrum (Bruker AMX360 instrument at 360.13 MHz and 298 K) of a 10 mM 1:1 BLM–Fe(II) sample in  $\text{D}_2\text{O}$  covering the diamagnetic region. (B) Diamagnetic region of the  $^1\text{H-NMR}$  512-scan spectrum of Fe(II)–BLM collected at 276 K.

starting point the assignments of Pillai et al. (1980) which were based solely on saturation transfer experiments. One- and two-dimensional NOE experiments were attempted but were unsuccessful because the molecular mass of the complex ( $\sim 1500$  Da) falls into the range where NOE effects are minimal (Neuhaus & Williamson, 1989).

*C-Terminal Amine, Bithiazole (BITH), and Threonine (THR) Assignments.* The COSY spectrum of the 1:1 BLM–Fe(II) sample covering the diamagnetic region is shown in Figure 3A. The NMR signal at 6.2 ppm attributed to the THR  $\text{C}^\alpha\text{H}$  proton by an ST experiment has a COSY connection with another feature located at 5.2 ppm (cross-peak a), which in turn is connected to a resonance among a group of signals between 2 and 2.5 ppm (cross-peak b). These latter signals can be resolved into three resonances by lowering the sample temperature to 276 K (Figure 3B signals g–i), the two at 2.1 and 2.3 ppm arising from  $\text{CH}_3$  groups. A COSY map obtained at this temperature (data not shown) shows that the feature at 5.2 ppm (shifted to 5.1 ppm at 276 K) is connected to the  $\text{CH}_3$  signal at 2.3 ppm. This  $\text{CHCHCH}_3$  spin system at 6.2, 5.2, and 2.3 ppm can thus be assigned to the THR  $\text{C}^\alpha\text{H}$ ,  $\text{C}^\beta\text{H}$ , and  $\text{C}^\beta\text{CH}_3$  protons, respectively. The fact that the THR protons shift only slightly when BLM binds Fe(II), together with their long  $T_1$  values (Table 1), indicates that these protons are not close to the paramagnetic Fe(II) center. In addition, the COSY spectrum of a 1:1 BLM–Fe(II) sample in  $\text{H}_2\text{O}$  shows a cross-peak between the THR  $\text{C}^\alpha\text{H}$  proton (6.2 ppm) and a solvent exchangeable signal at 15.0 ppm which can be assigned to the THR NH proton (Figure 4A, cross-signal a). The facile observation of the NH signal indicates that the peptide bond

Table 1: Summary of the Resonance Positions, Relaxation Times,  $T_1$ , and Calculated Proton–Metal Distances for the Protons in Fe(II)BLM at pH 6.5

peak position (ppm)		$T_1$ (ms)		ST (ppm)	assignments	$H_i$ –Fe (Å) <sup>a</sup>	$H_i$ –Co (Å) <sup>b</sup>
298 K	281 K	298 K	281 K				
206	225	1.2	1.3	<i>c</i>	HIST C <sup>α</sup> H	3.6	3.9
204	217	2.8	2.8	2.50	1/2 ALA C <sup>β</sup> H <sub>2</sub>	4.1	3.8
153	<i>d</i>	<0.8	–	<i>c</i>	PYR C <sup>β</sup> H	<3.1	3.0
127	142	1.5	1.7	3.73	ALA C <sup>α</sup> H	3.7	3.7
108	120	0.8	1	2.02	1/2 ALA C <sup>β</sup> H <sub>2</sub>	3.4	3.2
121	<i>d</i>	<0.8	–	8.30	HIST C2H	<3.1	3.2
66.5	–	–	–	np	HIST N3H	–	5.0
42.3	47.3	10.0	9.8	7.40	HIST C4H	5.0	5.1
–17.3	–20.1	3.1	5.0	4.72	HIST C <sup>β</sup> H	4.4	4.4
44.9	50.3	7.9	7.8	2.67	1/2 PYR C <sup>α</sup> H	4.8	4.9
32.1	37.9	5.8	5.9	2.64	1/2 PYR C <sup>α</sup> H	4.6	4.6
2.1 <sup>e</sup>	–	<i>f</i>	–	–	PYR CH <sub>3</sub>	–	5.7
14.0	–	–	–	np	PYR CONH <sub>2</sub>	–	5.8
10.1	–	–	–	np	PYR CONH <sub>2</sub>	–	6.4
12.9	14.8	32.8	35.3	1.10	VAL C <sup>α</sup> CH <sub>3</sub>	6.2	5.7
37.8	46.1	3.1	3.6	2.52	VAL C <sup>α</sup> H	4.2	3.8
24.8	26.9	7.6	7.0	3.74	VAL C <sup>β</sup> H	4.7	4.5
20.9	23.0	18.2	17.8	3.88	VAL C <sup>γ</sup> H	5.5	5.6
8.1	8.5	23.5	22.7	1.15	VAL C <sup>γ</sup> CH <sub>3</sub>	5.8	5.8
6.2	6.3	110.2	107.5	np	THR C <sup>α</sup> H	7.6	6.8
5.2	5.8	210.1	205.3	np	THR C <sup>β</sup> H	8.3	6.6
2.3 <sup>e</sup>	–	<i>f</i>	–	–	THR CH <sub>3</sub>	–	6.0
15.0	–	–	–	np	THR NH	–	4.0
–7.5	–9.0	16.0	16.6	5.07	G-1	5.5	4.9
–4.7	–6.0	59.4	61.2	4.03	G-2	6.8	6.4
<i>g</i>	–2.36	–	71.3	np	G-3	7.0	7.0
3.6	–	–	–	np	M-2, M-3, or G-4	–	–
–5.4	–6.9	15.3	15.9	3.94	G-5	5.4	5.7
1.5	1.5	106.0	100.0	np	G-6	7.4	7.4
2.3	2.5	115.0	105.0	np	G-6	7.4	8.2
<i>g</i>	–1.38	–	78.8	np	M-1	7.1	6.5
<i>g</i>	–2.10	–	90.9	np	M-2, M-3, or G-4	7.2	–
<i>g</i>	–2.40	–	106.5	np	M-2, M-3, or G-4	7.4	–
<i>g</i>	–2.48	–	111.8	np	M-4	7.5	7.2
–12.7	–14.9	22.1	23.9	3.78	M-5	5.8	5.8
<i>g</i>	–2.23	–	141.0	np	M-6	7.8	8.7
<i>g</i>	–2.68	–	133.3	np	M-6	7.7	8.0

<sup>a</sup> Data derived from the present study. The  $H_i$ –Fe(II) distances shown are calculated from eq 2 where the relaxation times ( $T_1$ 's) of the protons in Fe(II)BLM measured at 281 K were used. This temperature was selected since the –1.4 and –3 ppm cluster of resonances can be better resolved. The proton–metal distance and measured  $T_1$  for the C4H proton in the imidazole ring were the reference values used in eq 2, since the imidazole ring is rigid and, when bound to Fe(II), its C4H proton displays typically proton–metal distances of ~5 Å in model complexes. <sup>b</sup> From Wu et al. (1996a). <sup>c</sup> The diamagnetic responses to irradiation of these signals could not be detected in the ST experiments. <sup>d</sup> Broadened beyond detection at 281 K. <sup>e</sup> Signals resolved at 276 K. <sup>f</sup> Relaxation times,  $T_1$ , for these protons were not measured in Fe(II)BLM due to the overlap of the signals in the diamagnetic region of the spectrum at 298 and 281 K. <sup>g</sup> Cluster of poorly resolved resonances which are better resolved at 281 K. np is not performed. Saturation transfer experiments were not performed on these signals.

connecting the THR and VAL units does not participate in binding to the Fe(II) center.

Also present in the COSY spectrum in Figure 3A are cross-peaks that connect the (CH<sub>2</sub>)<sub>n</sub> resonances of the dimethylsulfonium (BLM-A<sub>2</sub>) (3.6, 3.4, and 2.2 ppm, cross-signals c and d) and agmatine (BLM-B<sub>2</sub>) (3.4, 3.3, and 1.7 ppm, cross-peaks e and f) moieties. Comparison of the COSY spectrum in Figure 3A with similar spectra acquired by Haasnoot et al. (1984) for apbleomycin indicates that the protons in these moieties are not affected by the binding of Fe(II) to BLM. Similarly, the chemical shifts of the two methylenes and the two ring protons in the bithiazole moiety are consistent with the findings of other studies of diamagnetic metallobleomycins which establish that the bithiazole tail is not involved in metal complexation by the antibiotic (Stubbe & Kozarich, 1987; Dabrowiak, 1982).

**α-Methylvalerate (VAL) Assignments.** ST experiments performed on a 2:1 BLM–Fe(II) sample in D<sub>2</sub>O by Pillai et al. (1980) and in this work (Table 1) have allowed the assignments of the signals at 37.8, 24.8, 20.9, and 8.1 ppm

(Figure 2A) to the VAL C<sup>α</sup>H, VAL C<sup>β</sup>H, VAL C<sup>γ</sup>H, and VAL C<sup>γ</sup>CH<sub>3</sub> protons, respectively. In addition, the 8.1 ppm resonance, which has an intensity of three protons, shows a TOCSY cross-peak to the resonance at 20.9 ppm, which is in turn correlated to the 24.8 ppm resonance (Figure 5A, cross-peaks a and b). These results show the presence of another CHCHCH<sub>3</sub> unit, which we associate with the C<sup>β</sup>H, C<sup>γ</sup>H, and C<sup>γ</sup>CH<sub>3</sub> protons of the VAL moiety.

In principle, the VAL C<sup>β</sup>H (24.8 ppm) peak should be correlated to the VAL C<sup>α</sup>H signal at 37.8 ppm. However, this correlation has not been detected in any of the NMR experiments described in the present work. As can be seen from Figure 5, the correlation (cross-peak a) between the signals at 24.8 ppm (C<sup>β</sup>H,  $T_1$  = 7.6 ms) and 20.9 ppm (C<sup>γ</sup>H,

<sup>2</sup> The intensity of a COSY cross-peak is in part dependent on the transverse relaxation times,  $T_2$ , of the correlated signals. While  $T_2$  values can be estimated from the line widths,  $T_1$  values can be more readily obtained by inversion–recovery measurements. Since  $T_2 \leq T_1$ , the  $T_1$  value can serve as a reliable index for the size of  $T_2$  in the context of these experiments.

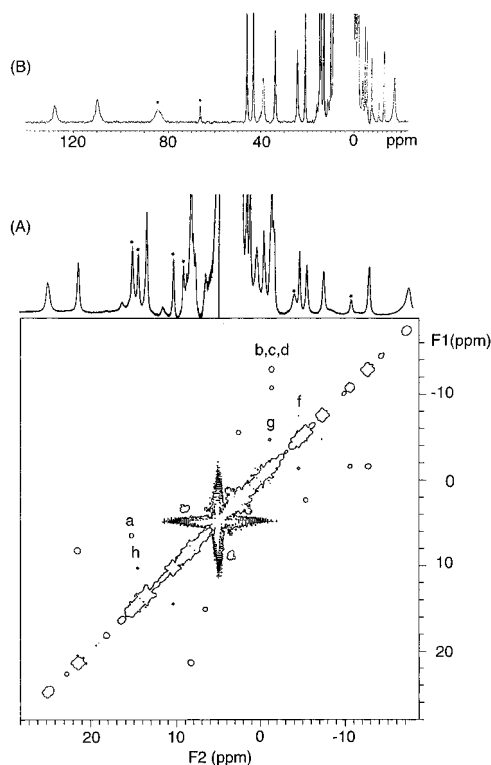


FIGURE 4: (A)  $^1\text{H}$ -COSY 400-scan spectrum (Bruker AMX360 instrument at 360.13 MHz and 298 K) of a 10 mM 1:1 BLM–Fe(II) sample in  $\text{H}_2\text{O}$ . A one-dimensional NMR spectrum of Fe(II)BLM in  $\text{H}_2\text{O}$  is shown along the first dimension. Asterisks (\*) indicate signals generated by  $\text{H}_2\text{O}$  exchangeable NH protons. (B) Region between 140 and  $-20$  ppm of the 512-scan spectrum of Fe(II)BLM in  $\text{H}_2\text{O}$  showing the signals at 84.3 and 66.4 ppm generated by solvent exchangeable protons.

$T_1 = 18.2$  ms) is weaker than that (cross-peak b) between the signals at 20.9 and 8.1 ppm ( $\text{C}^\gamma\text{CH}_3$ ,  $T_1 = 23.5$  ms) due to the faster relaxation behavior of the 24.8 ppm signal (Table 1).<sup>2</sup> Since the feature at 37.8 ppm has an even shorter  $T_1$  (3.1 ms), it is unlikely that a connection between the features at 37.8 and 24.8 ppm can be observed. Furthermore, no COSY or TOCSY correlations between these two protons could be detected in the NMR studies of the diamagnetic HOO–Co(III)BLM complex; this absence was attributed to the small coupling constant ( $J = 1.8 \pm 1.2$  Hz) between the  $\alpha$ - and  $\beta$ -protons of the VAL fragment (Wu et al., 1996b), which further renders unobservable the correlation between paramagnetically shifted peaks. The lack of correlations involving the 37.8 ppm signal breaks the pattern of connections that otherwise should be observed for the VAL spin system and does not allow the confirmation of the assignment of the VAL  $\text{C}^\alpha\text{H}$  proton made through ST. In these experiments, irradiation of the feature at 37.8 ppm elicits a response from a signal at 2.5 ppm in apo-bleomycin which can be attributed to either of the protons in the PYR  $\text{C}^\beta\text{H}$ , ALA  $\text{C}^\beta\text{H}_2$ , or VAL  $\text{C}^\alpha\text{H}$  groups (Haasnoot et al., 1984). Since the secondary amine in the  $\beta$ -aminoalanine moiety is by consensus coordinated to the metal center (Stubbe & Kozarich, 1987; Dabrowiak, 1982), the NMR features for the methylene protons in ALA and the  $\beta$ -proton in PYR are expected to have much larger isotropic shifts and shorter  $T_1$  values than the 37.8 ppm signal. This situation leaves the VAL  $\text{C}^\alpha\text{H}$  as the only choice for the assignment of the feature at 37.8 ppm.

The  $\text{CH}_3$  signal at 12.9 ppm is assigned to the VAL  $\text{C}^\alpha\text{CH}_3$  group on the basis of its ST connections to a  $\text{CH}_3$  signal at 1.10 ppm. Unfortunately, no cross-peak between the VAL  $\text{C}^\alpha\text{CH}_3$  and the VAL  $\text{C}^\alpha\text{H}$  protons can be observed that would have corroborated this assignment, due to the short  $T_1$  of the latter. There are four  $\text{CH}_3$  groups in the BLM molecule, two of which have already been associated with signals at 2.3 ppm (at 276 K) (THR  $\text{C}^\beta\text{CH}_3$ ) and 8.1 ppm (VAL  $\text{C}^\gamma\text{CH}_3$ ) (vide supra). The third  $\text{CH}_3$  group is on the pyrimidine ring and has a shift of 2.004 ppm in apo-BLM (Haasnoot et al., 1984), a value incompatible with the ST results for the 12.9 ppm resonance. This leaves the VAL  $\text{C}^\alpha\text{CH}_3$  group as the only possible assignment for the 12.9 ppm signal.

**$\beta$ -Hydroxyhistidine (HIST) Assignments.** The three aromatic HIST protons can be assigned. The signal located at 42.3 ppm (Figure 2A) shows an ST response at 7.4 ppm, a chemical shift value associated with the imidazole ring C4H proton (Haasnoot et al., 1984; Pillai et al., 1980). The isotropic shift of the HIST C4H proton and its relaxation time, 10.0 ms, are typical for the C4H proton of an imidazole ring coordinated to an iron(II) center through the N1 nitrogen (Ming et al., 1992, 1994). The N3H proton of such a coordinated imidazole is expected near 60–70 ppm (Wu & Kurtz, 1989; Scarrow et al., 1990; Wang et al., 1992; Elgren et al., 1994; Bertini et al., 1993; Maroney et al., 1986) and is indeed located at 66.5 ppm in the spectrum of Fe(II)BLM in  $\text{H}_2\text{O}$  (Figure 4B). A third signal at 121 ppm is connected by ST response to a signal at 8.3 ppm. The position of the diamagnetic response identifies it as an aromatic proton (Haasnoot et al., 1984), and the large paramagnetic shift and short  $T_1$  value in Fe(II)BLM indicate that it is close to a ligating atom. These properties unequivocally assign it to the HIST C2H proton.

The signals arising from the HIST  $\text{C}^\alpha\text{H}$  and  $\text{C}^\beta\text{H}$  protons are more difficult to assign. These protons are respectively located at 5.06 and 5.36 ppm in apo-BLM (Haasnoot et al., 1984), a relatively uncrowded region of the spectrum, so their paramagnetically shifted counterparts may be recognized by ST experiments. In this manner, the signals at  $-7.5$  and  $-17.3$  ppm were singled out. However, the  $-7.5$  ppm feature has two-dimensional connections that invalidate its assignment to any proton in the HIST moiety and can be attributed to the G-1 proton (vide infra). This leaves only the signal at  $-17.3$  ppm to be associated with either the HIST  $\text{C}^\alpha\text{H}$  or  $\text{C}^\beta\text{H}$  proton. Due to the likely coordination of both HIST imidazole and amide nitrogens to the metal center, the  $\text{C}^\alpha\text{H}$  proton like the C2H proton is expected to exhibit a very short  $T_1$  and give rise to one of the six signals in the 210–90 ppm region of the spectrum (Figure 2A). Thus, the signal at  $-17.3$  ppm may be assigned to the HIST  $\text{C}^\beta\text{H}$  proton. Unfortunately, the short  $T_1$ 's of the  $\text{C}^\alpha\text{H}$  and  $\text{C}^\beta\text{H}$  protons preclude the observation of a COSY cross-peak that could have facilitated their assignment.

**Pyrimidinylpropionamide (PYR) Assignments.** The ST results indicate that the features at 44.9 and 32.1 ppm (Figure 2A) can be attributed to the geminal PYR  $\alpha$ -methylene protons (Table 1). This is confirmed by the appearance of a cross-peak between these two signals in the COSY spectrum shown in Figure 5B (cross-signal c). The magnitudes of the isotropic shifts of the PYR methylene protons are consistent with the coordination to the iron of the secondary amine in the ALA moiety (Pillai et al., 1980).

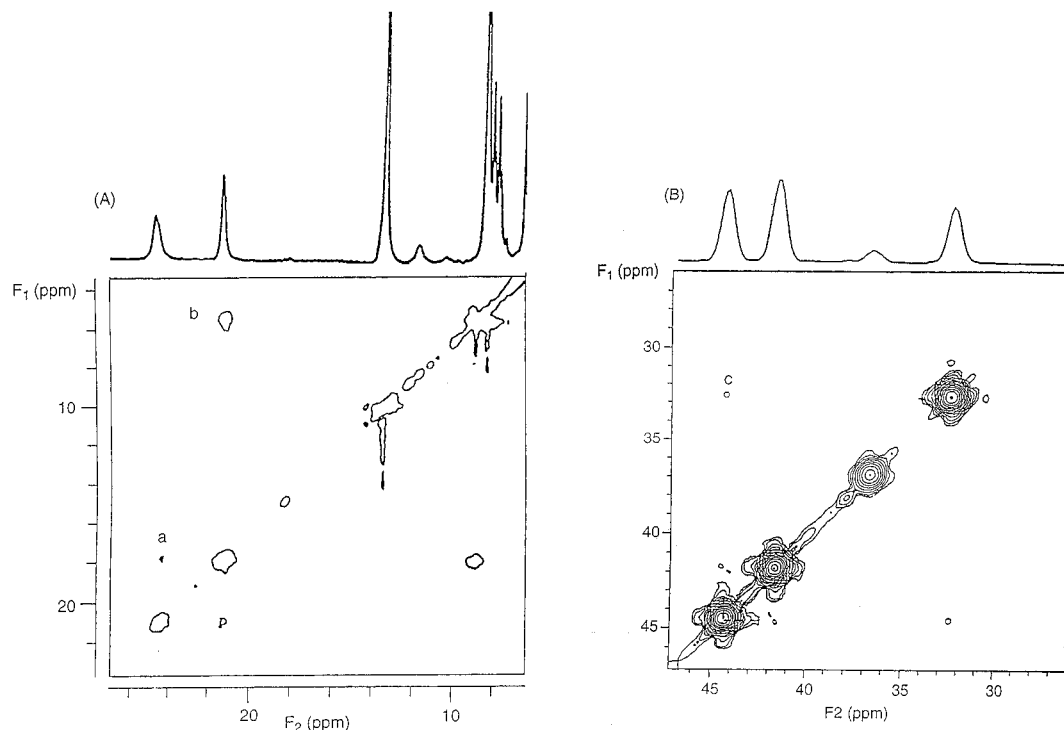


FIGURE 5: Two-dimensional  $^1\text{H}$ -NMR spectra showing the cross-peaks that allowed the identification of the signals generated by protons in the VAL and PYR moieties. (A)  $^1\text{H}$ -TOCSY 200-scan spectrum (Bruker AMX360 instrument at 360.13 MHz and 298 K) of a 10 mM 1:1 BLM-Fe(II) sample in  $\text{D}_2\text{O}$  showing the cross-peaks connecting the VAL  $\text{C}'\text{H}$  and VAL  $\text{C}'\text{H}$  (cross-peak a) and VAL  $\text{C}'\text{H}$  and VAL  $\text{C}'\text{CH}_3$  (cross-peak b) protons. (B)  $^1\text{H}$ -COSY 2000-scan spectrum (Varian VXR500 instrument at 499.88 MHz and 298 K) of a 10 mM 1:1 BLM-Fe(II) sample in  $\text{D}_2\text{O}$  showing the cross-peak connecting the signals at 44.9 and 32.1 ppm (cross-peak c). These signals have been assigned to the PYR methylene group.

The  $T_1$ 's for these features (Table 1) as well as their positions in the NMR spectrum are appropriate for protons located three bonds away from a ligation site (Ming et al., 1994; Wang et al., 1993). However, the signal derived from the PYR  $\text{CH}_3$  group is rather difficult to identify due to the absence of nearby non-solvent exchangeable protons. The only  $\text{CH}_3$  signal left unassigned in the spectrum is the one at 2.1 ppm (at 276 K) (Figure 3B, signal h). While the lack of a significant shift is unexpected, this observation is consistent with the behavior of the pyrimidine methyl group observed in Co(II)BLM (T. E. Lehmann and L. Que, Jr., to be published).

**Gulose (G) and Mannose (M) Assignments.** With the assignments made thus far, the major subset of unassigned signals consists of the resonances derived from the protons in the sugar moieties, gulose and mannose. ST experiments indicate that almost all of the isotropically shifted signals in the region between  $-0.6$  and  $-15.0$  ppm (Figure 2B) come from the sugar protons. The ST responses obtained upon irradiation of these signals are located between 3.78 and 5.07 ppm (Table 1), coinciding with the region, 3.4–5.2 ppm, where the sugar resonances are positioned in the NMR spectrum of apobleomycin (Haasnoot et al., 1984). Further support for the assignments of these signals comes from HMQC experiments (Figure 6). Fourteen  $^1\text{H}$ -NMR signals between 4 and  $-13$  ppm are correlated with twelve  $^{13}\text{C}$ -NMR signals located between 63 and 94 ppm (cross-peaks a–n). These carbon signals fall within the 60–100 ppm region where the sugar carbons are found in diamagnetic adducts of BLM (Wu et al., 1996a; Akkerman et al., 1988, 1990). Two of the  $^{13}\text{C}$  signals have shifts of ca. 90 ppm, identifying them as the anomeric sugar carbons; correspondingly, the  $^1\text{H}$  features at  $-7.5$  and  $-1.38$  ppm are the

anomeric sugar protons. Two other  $^{13}\text{C}$  signals are each correlated to a pair of protons, identifying them as the sugar  $\text{C}6$ 's.

In principle, the sugar protons could be assigned by a network of connectivity within each sugar moiety. Indeed, such networks have been observed in the COSY spectra of apo-BLM and diamagnetic metallobleomycins (Akkerman et al., 1988; Haasnoot et al., 1984). However, the shorter relaxation times of these protons due to the presence of the paramagnetic center have made a number of expected COSY cross-peaks more difficult to detect. By examining the COSY spectra of this region, we have been able to identify three subsets of signals arising from the sugar moieties.

One network of three signals can be established in Figure 3A by correlating the features at  $-5.4$  ppm to that at 2.3 ppm (cross-peak j) and in turn to that at 1.5 ppm (cross-peak k). Since the latter two are correlated with one carbon (Figure 6A, cross-peaks a and b), they must be the geminal protons on a sugar  $\text{C}6$  carbon, and this three-signal network must be associated with a  $\text{C}5\text{H}-\text{C}6\text{H}_2$  spin subsystem.

Another network of connected signals (cross-peaks b–d) is present in Figure 4A but more readily observed in Figure 7 obtained at 281 K to achieve better resolution of the features in the region between  $-0.6$  and  $-3$  ppm (Figure 2B). The resonance at  $-14.9$  ppm ( $-12.7$  ppm at 298 K) correlates with three features, more strongly to the two at  $-2.23$  (Figure 7, cross-peak b) and  $-2.48$  ppm (Figure 7, cross-peak c) and more weakly to the one at  $-2.68$  ppm (Figure 7, cross-peak d). The signals at  $-2.23$  and  $-2.68$  ppm are in turn connected by a strong cross-peak (e), suggestive of another geminal pair; both are correlated to the same carbon atom in the HMQC spectra (Figure 6A, cross-peaks c and d). The only sugar proton that can have

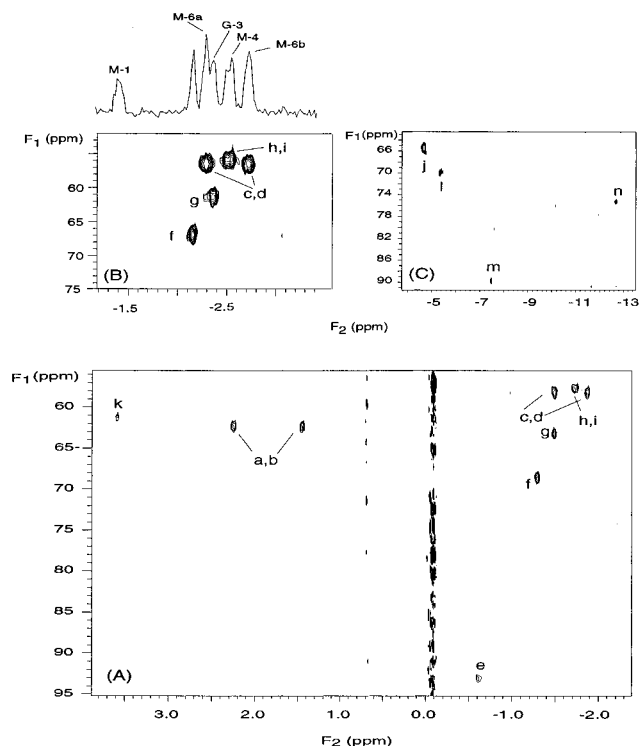


FIGURE 6: HMQC spectra (Varian VXR500 instrument at 499.88 MHz at 298 K) of the 1:1 BLM–Fe(II) sample in D<sub>2</sub>O. (A) This spectrum, collected at 298 K, was the sum of 100 scans obtained with a 300 ms relaxation delay; (B) this spectrum was collected at 298 K. Due to the short  $T_1$ 's of the protons involved, this spectrum was the sum of 250 scans acquired with a relaxation delay of 20 ms. (C) This spectrum was collected at 281 K to take advantage of the better resolution in the cluster of <sup>1</sup>H resonances between –2 and –3 ppm. This spectrum was the sum of 100 scans obtained with a relaxation delay of 300 ms.

three connections is the one at C5 which can couple with protons at C4 and C6. Therefore, the set of signals at –14.9, –2.23, –2.48, and –2.68 ppm must be assigned to a C4H–C5H–C6H<sub>2</sub> spin subsystem that is distinct from the previously identified C5H–C6H<sub>2</sub> network.

A third network can be observed in Figure 4A, where the resonance at –7.5 ppm is correlated with the signal at –4.7 ppm (cross-peak f), which in turn is connected to the resonance at approximately –1 ppm (–2.36 ppm at 281 K; Figure 7, cross-peak g). Since the –7.5 ppm signal is identified as an anomeric sugar proton on the basis of its ST response near 5 ppm and its HMQC connection to a <sup>13</sup>C signal at 90 ppm (Figure 6B, cross-peak m), this third network must be associated with the C1H–C2H–C3H spin subsystem of either mannose or gulose.

The arguments offered so far allow the assignment of the –0.6 to –15 ppm signals (Figure 2B) to the sugar protons and the identification of some of the spin subsystems in these moieties. Specific assignments of these spin subsystems to either sugar based on the ST results are not possible at this point, due to the significant overlap and similarity in chemical shift exhibited by the signals generated by the sugar protons in apo-BLM (Haasnoot et al., 1984). In this regard, the NMR-generated solution structures of HOO–Co(III)BLM (Wu et al., 1996a,b) have provided a means of more specifically assigning the signals referred to above through structural correlations between the relaxation times,  $T_1$ 's, of some of the protons in Fe(II)BLM and the proton–metal distances of the corresponding protons in the HOO–Co(III)–

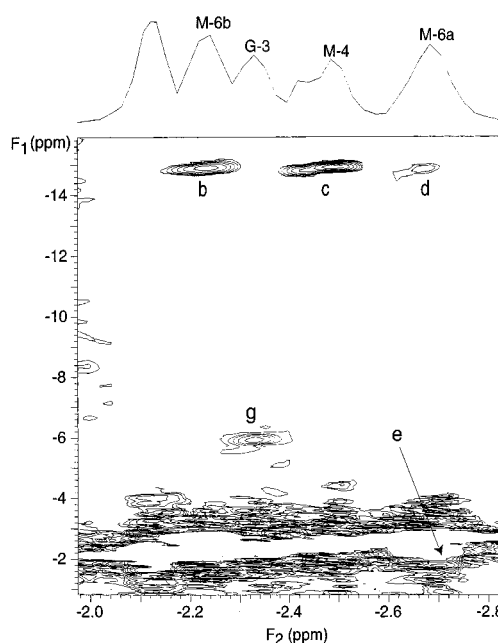


FIGURE 7: Expansion of the –2 to –3 ppm region of the <sup>1</sup>H-COSY 2000-scan spectrum (Varian VXR500 instrument at 499.88 MHz at 281 K) of a 10 mM 1:1 BLM–Fe(II) sample in D<sub>2</sub>O covering the region between –1 and –16 ppm. This spectrum was acquired at 281 K to overcome the extensive overlap shown by the signals of the protons in the sugar moieties.

BLM structure. These correlations have allowed the assignments of the three networks of connected signals discussed before to the gulose C5H–C6H<sub>2</sub>, mannose C4H–C5H–C6H<sub>2</sub>, and gulose C1H–C2H–C3H, respectively (vide infra). This leaves the signals at 3.6, –2.10, and –2.40 ppm unassigned, which must arise from the G-4, M-2, and M-3 protons.

*Coordination Environment of the Metal Center in Fe(II)–BLM.* The nature of the atoms ligating to the metal centers of metallobleomycins has been a matter of some discussion among the various investigators in this field. Our observations allow us to favor one particular ligand set on the basis of the number of signals observed in the 90–210 ppm region. Due to their large paramagnetic shifts and their very short  $T_1$ 's, these signals must arise from CH protons that are two bonds away from the ligating atoms. Analogous protons in model complexes such as [Fe(II)(TPA)SAr] (Zang & Que, 1995), [Fe(II)<sub>2</sub>(N-Et-HPTB)(OBz)](BF<sub>4</sub>)<sub>2</sub> (Dong et al., 1993), [Fe(II)Zn(II)BPMP(O<sub>2</sub>CCH<sub>2</sub>CH<sub>3</sub>)<sub>2</sub>](BPh<sub>4</sub>) (Wang et al., 1993), [Fe(II)<sub>2</sub>(TPA)<sub>2</sub>(O<sub>2</sub>CCH<sub>3</sub>)<sub>2</sub>](BPh<sub>4</sub>)<sub>2</sub> (Ménage et al., 1992), and [Fe(II)<sub>2</sub>(BPMP)[O<sub>2</sub>P(OPh)<sub>2</sub>]<sub>2</sub>](BF<sub>4</sub>) (Ming et al., 1992) indeed exhibit these NMR properties. There are six signals in this region, all with  $T_1$ 's of <3 ms. The appearance of six such signals is consistent only with the following ligand set: the primary and secondary amine nitrogens of ALA, the pyrimidine N5, and the HIST imidazole and amidate nitrogens. This set of ligands is also favored by Wu et al. (1996a) for HOO–Co(III)BLM. Assuming this ligand set, ST experiments on these broad features allowed us to assign the features at 204, 108, 127, and 121 ppm to the ALA C<sup>β</sup>H<sub>2</sub>, ALA C<sup>α</sup>H, and HIST C2H protons, respectively (Table 1). The 206 and 153 ppm could not be correlated with their diamagnetic counterparts, because the very short  $T_1$ 's (<1 ms) of these paramagnetic features engendered weak ST responses which in turn were obscured by their proximity

to the HDO signal; these two are thus assigned to the PYR C $\beta$ H and HIST C $\alpha$ H protons by default.

The alternative ligand set favored by Pillai et al. (1980), in which the ALA primary amine is replaced with the carbamoyl moiety of the mannose, would give rise to only five protons two bonds away from a ligating atom. The ALA C $\alpha$ H proton would instead become three bonds away from a ligating atom and should then have NMR properties similar to those of the PYR C $\alpha$ H<sub>2</sub> protons which are found at 44.9 and 32.1 ppm and have  $T_1$ 's of 8 and 6 ms, respectively. Therefore, the ALA C $\alpha$ H proton should give rise to a signal positioned in that region with a relaxation time of approximately 7 ms and showing a ST response around 4.07 ppm when irradiated. No such signal has been observed.

The coordination of the ALA primary amine is also consistent with the NMR spectrum of Fe(II)BLM in H<sub>2</sub>O which shows only one pair of solvent exchangeable NH protons at 14.0 and 10.1 ppm correlated via a COSY cross-peak (Figure 4A, cross-signal h). There are five NH<sub>2</sub> groups in BLM: the carbamoyl NH<sub>2</sub> group in the mannose moiety, two primary amines (on PYR and ALA), and two amides (on PYR and ALA) (Figure 1). Of these, only the last two can give rise to pairs of solvent exchangeable resonances. Primary aliphatic amine protons typically exchange rapidly with solvent and would not be observed as separate resonances. Only one NMR signal from the PYR ring NH<sub>2</sub> group has been detected in the NMR studies of apo-BLM (Haasnoot et al., 1984) and the Zn (Akkerman et al., 1988b) and Fe(II)-CO (Akkerman et al., 1990) adducts of the drug, indicating that these protons are effectively equivalent. NMR studies of apo-, Zn(II)-, and Fe(II)(CO)BLM have also shown that the protons of the carbamoyl NH<sub>2</sub> group generate very broad signals due to rapid exchange with solvent protons. The broadening of these signals would be even worse in the presence of Fe(II). For the reasons described above, these three NH<sub>2</sub> groups are discarded as possible candidates for the 14.0 and 10.1 ppm pair of exchangeable signals. If the carbamoyl group were coordinated to the metal center, the amide protons in the PYR and ALA moieties would all be six bonds away from the metal center. This should result in the detection of two sets of paired exchangeable resonances for the two CONH<sub>2</sub> groups, which should be related by COSY peaks. The fact that only one set of COSY-connected solvent exchangeable resonances is observed in Figure 4A (signals at 14.0 and 10.1 ppm, cross-peak h) is best rationalized by the ligation of the primary amine in ALA. Due to the close proximity of the ALA CONH<sub>2</sub> protons to the metal center, only the PYR CONH<sub>2</sub> protons can give rise to the 14.0 and 10.1 ppm pair. The evidence discussed above then favors the coordination of the ALA NH<sub>2</sub> nitrogen to the metal center in Fe(II)BLM, rather than the participation of the carbamoyl group in metal complexation.

*Three-Dimensional Folding of the BLM Segments around the Fe(II) Center.* With most of the paramagnetically shifted resonances assigned, we can use the  $T_1$  values measured for the assigned protons to calculate Fe(II)–proton distances and postulate what structure Fe(II)BLM adopts in solution. This analysis is based on eq 1 which describes the effects of dipolar relaxation and relates the  $T_1$  of a proton to its distance from the paramagnetic metal center (Bertini & Luchinat, 1986; La Mar & de Ropp, 1993).

$$\frac{1}{T_1} = \frac{2(g\beta\gamma)^2 S(S+1) f(T_{1e})}{15(r_M)^6} \quad (1)$$

In eq 1,  $g$  is the Lande  $g$  factor for the metal,  $\beta$  is the Bohr magneton,  $\gamma$  is the nuclear magnetogyric ratio,  $r_M$  is the proton–metal distance,  $S$  is the electronic spin angular momentum quantum number, and  $f(T_{1e})$  is a correlation function dependent on the electronic relaxation time  $T_{1e}$ . For two nonequivalent nuclei  $j$  and  $k$  in the same molecule, the corresponding equations for  $1/T_{1j}$  and  $1/T_{1k}$  can be combined to obtain

$$r_{Mj} = r_{Mk} (T_{1j}/T_{1k})^{1/6} \quad (2)$$

If  $r_{Mk}$  and  $T_{1k}$  for nucleus  $k$  are known, eq 2 leads to  $r_{Mj}$ . The proton–metal distances calculated for the protons in Fe(II)BLM are shown in Table 1. In these calculations, the proton–metal distance for the C4H proton in the imidazole ring was the reference value used in eq 2, since the imidazole ring is rigid and, when bound to Fe(II), its C4H proton typically displays proton–metal distances of  $\sim 5$  Å in model complexes (Tolman et al., 1991; Mandon et al., 1990; Spek et al., 1983).

A solution structure for HOO-Co(III)BLM has recently been deduced from two-dimensional NMR methods (Wu et al., 1996a) (Figure 8A). In Figure 8B, the  $T_1$ 's of the assigned paramagnetically shifted protons in Fe(II)BLM are plotted versus the proton–metal distances of the respective protons in HOO-Co(III)BLM to determine whether the two complexes adopt similar structures. The HOO-Co(III)BLM–Fe(II)BLM data were then fitted to an equation of the form  $r = a(T_1)^b$  (according to eq 2 where  $b = 1/6$ ), and a very good fit was obtained (correlation coefficient of 0.97). The fit in Figure 8B was obtained with the <sup>1</sup>H-NMR signals of the three networks of correlated signals identified previously for the sugar moieties assigned to gulose C5H–C6H<sub>2</sub>, mannose C4H–C5H–C6H<sub>2</sub>, and gulose C1H–C2H–C3H, respectively. When the mannose and gulose assignments were interchanged, the HOO-Co(III)BLM:Fe(II)BLM correlation was significantly inferior (correlation coefficient of <0.5), supporting the assignments listed in Table 1.

The quality of the fit shown in Figure 8B indicates that the arrangement of the BLM segments bearing these protons is very similar in both Fe(II)- and Co(III)BLM. Therefore, the HOO-Co(III)BLM:Fe(II)BLM correlation supports the set of ligands deduced from the analysis of the NMR data presented in this study and previously proposed by other workers in the field (Stubbe & Kozarich, 1987; Dabrowiak, 1982). This analysis enables us to exclude the M moiety from the first coordination sphere of the Fe(II) in Fe(II)BLM. Analysis of the proton–metal distances derived from the NMR-generated structure for HOO-Co(III)BLM bound to [d(CCAGGCCTGG)]<sub>2</sub> (Wu et al., 1996b) indicates that the mannose moiety alters its conformation significantly upon DNA binding. When the coordinates of the DNA-bound structure were used to carry out the HOO-Co(III)BLM:Fe(II)BLM correlation, a good fit was obtained only if the mannose protons were excluded from the data sets (data not shown), demonstrating that the conformation of this residue in the DNA-bound structure is inconsistent with our NMR data. The mannose moiety thus has a considerably larger flexibility when compared with the other BLM fragments.



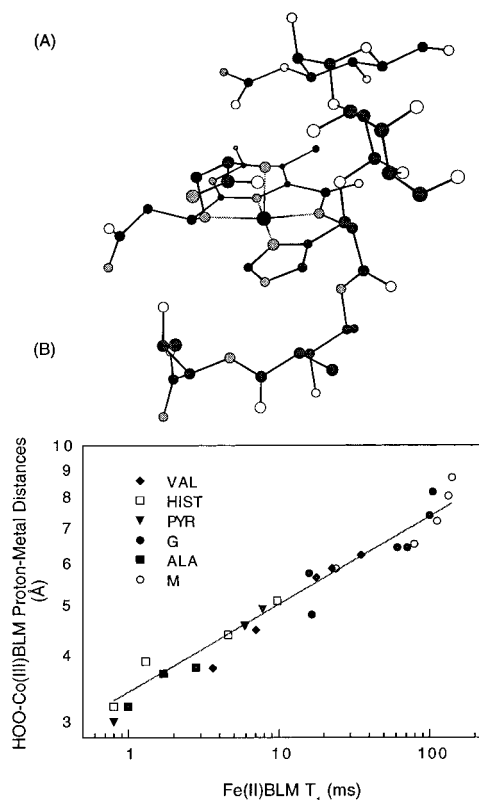


FIGURE 8: (A) NMR-generated structure for HOO-Co(III)BLM (Wu et al., 1996a) (the bithiazole tail has been removed for clarity). A similar wrapping of the BLM segments around the metal center is proposed for Fe(II)BLM on the basis of the analysis of the NMR data generated in the present study, in conjunction with the results of the HOO-Co(III)BLM–Fe(II)BLM structural correlation. (B) Correlation between the  $T_1$  values from Fe(II)BLM and the proton–metal distances from HOO-Co(III)BLM (Wu et al., 1996a). The correlation coefficient obtained from the fitting of the HOO-Co(III)BLM–Fe(II)BLM data sets with eq 2 was 0.97.

These observations are consistent with the results of Boger et al. (1985) showing that gulose (but not mannose) plays an important role in DNA cleavage by Fe(II)BLM.

In summary, the present NMR study has allowed us to identify the ligands to the metal center in the Fe(II) adduct of BLM as derived from the  $\beta$ -aminoalanine (primary and secondary amines), the pyrimidinylpropionamide (pyrimidine ring), and the  $\beta$ -hydroxyhistidine (amide nitrogen and imidazole ring) segments. The two-dimensional NMR techniques used have enabled us to identify many of the spin networks present in the NMR spectrum of the paramagnetic Fe(II)BLM and eliminate the earlier ambiguity in the assignments for the signals between  $-0.8$  and  $-20$  ppm (Figure 2B) (Pillai et al., 1980). The analysis of the NMR data indicates that the VAL and/or M segments do not participate in Fe(II) complexation. Therefore, the isotropic shifts exhibited by the protons in these fragments must be attributed to their close proximity to the paramagnetic Fe(II) ion. There is a close structural correlation between the Fe(II) and Co(III) adducts of BLM, indicating that these two congeners, both with the ability to cleave DNA, share the same set of ligands and adopt similar overall structures.

#### ACKNOWLEDGMENT

We thank Drs. A. J. Razel and S. J. Lucania of Bristol-Myers Squibb for generously providing us with Bleomycin. We are grateful to Prof. R. C. Holz (Utah State University)

for timely and helpful suggestions and Dr. Vikram Roongta (University of Minnesota NMR facilities) and Dr. Zhigang Wang (presently at The Pennsylvania State University) and Mr. Xiangdong Wei (University of South Florida) for assistance in data collection and analysis. Our gratitude also goes to Professor JoAnne Stubbe and Mr. Wei Wu (Massachusetts Institute of Technology) for sharing with us their structural data on HOO-Co(III)BLM prior to publication and for very useful discussions.

#### REFERENCES

- Absalon, M. J., Kozarich, J. W., & Stubbe, J. (1995a) *Biochemistry* 34, 2065–2075.
- Absalon, M. J., Wu, W., Kozarich, J. W., & Stubbe, J. (1995b) *Biochemistry* 34, 2076–2086.
- Akkerman, M. A. J., Haasnoot, A. G., & Hilbers, C. W. (1988) *Eur. J. Biochem.* 173, 211–225.
- Akkerman, M. A. J., Neijman, E. W. J. F., Wijmenga, S. S., Hilbers, C. W., & Bermel, W. (1990) *J. Am. Chem. Soc.* 112, 7462–7474.
- Antholine, W. E., Hyde, J. S., Saely, R. C., & Petering, D. H. (1984) *J. Biol. Chem.* 259, 4437–4440.
- Bertini, I., & Luchinat, C. (1986) *NMR of Paramagnetic Molecules in Biological Systems*, pp 19–45, Benjamin & Cummings Publishing Co., Inc., Menlo Park, CA.
- Bertini, I., Turano, P., & Vila, A. J. (1993) *Chem. Rev.* 93, 2833–2932.
- Boger, D. L., Teramoto, S., Honda, T., & Zhou, J. (1995) *J. Am. Chem. Soc.* 117, 7338–7343.
- Brown, S. J., & Mascharak, P. K. (1988) *J. Am. Chem. Soc.* 110, 1996–1997.
- Brown, S. J., Hudson, S. E., Stephan, D. W., & Mascharak, P. K. (1989) *Inorg. Chem.* 28, 468–477.
- Chen, D. M., Hawkins, B. L., & Glickson, J. D. (1977) *Biochemistry* 16, 2731–2738.
- Cullinam, E. B., Gawron, L. S., Rustum, Y. M., & Beerman, T. A. (1991) *Biochemistry* 30, 3055–3061.
- Dabrowiak, J. C. (1982) *Adv. Inorg. Chem.* 4, 69–113.
- Dabrowiak, J. C., & Tsukayama, M. (1981) *J. Am. Chem. Soc.* 103, 7543–7550.
- Dabrowiak, J. C., Greenaway, F. T., Longo, W. E., Van Hausen, M., & Crooke, S. T. (1978) *Biochim. Biophys. Acta* 517, 517–526.
- Dong, Y., Ménage, S., Brennan, B. A., Elgren, T. E., Jang, H. G., Pearce, L. L., & Que, L., Jr. (1993) *J. Am. Chem. Soc.* 115, 1851–1859.
- Elgren, T. E., Ming, L.-J., & Que, L., Jr. (1994) *Inorg. Chem.* 33, 891–894.
- Farinas, E., Tan, J. D., Baidya, N., & Mascharak, P. K. (1993) *J. Am. Chem. Soc.* 115, 2996–2997.
- Guajardo, R. J., & Mascharak, P. M. (1995) *Inorg. Chem.* 34, 802–808.
- Guajardo, R. J., Hudson, S. E., Brown, S. J., & Mascharak, P. K. (1993) *J. Am. Chem. Soc.* 115, 7971–7977.
- Gupta, R. K., Ferreti, J. A., & Caspary, W. J. (1979) *Biochem. Biophys. Res. Commun.* 89, 534–541.
- Haasnoot, C. A. G., Pandit, U. K., Kurk, C., & Hilbers, C. W. (1984) *J. Biomol. Struct. Dyn.* 2, 449–467.
- Hecht, S. M. (1986) *Acc. Chem. Res.* 19, 383–391.
- Itaka, Y., Nakamura, H., Nakatani, T., Muraoka, Y., Fujii, A., Takita, T., & Umezawa, H. (1978) *J. Antibiot.* 31, 1070–1072.
- La Mar, G., de Ropp, J. S. (1993) in *NMR of Paramagnetic Molecules* (Berliner, L. J., & Reuben, J., Eds.) pp 1–73, Plenum Press, New York.
- Lazo, J. S., & Sebti, S. M. (1989) in *Anticancer Drug Resistance* (Kessel, D., Ed.) pp 267–280, CRC Press, Boca Raton, FL.
- Manderville, R. A., Ellena, J. F., & Hecht, S. M. (1995) *J. Am. Chem. Soc.* 117, 7891–7903.
- Mandon, D., Ott-Woelfel, F., Fischer, J., Weiss, R., Bill, E., & Trautwein, A. X. (1990) *Inorg. Chem.* 29, 2442–2447.
- Maroney, M. J., Kurtz, D. M., Jr., Nocek, J. M., Pearce, L. L., & Que, L., Jr. (1986) *J. Am. Chem. Soc.* 108, 6871–6879.

- McGall, G. H., Rabow, L. E., Ashley, G. W., Wu, S. H., Kozarich, J. W., & Stubbe, J. (1992) *J. Am. Chem. Soc.* *114*, 4958–4967.
- Ménage, S., Zang, Y., Hendrich, M. P., & Que, L., Jr. (1992) *J. Am. Chem. Soc.* *114*, 7786–7792.
- Ming, L.-J., Jang, H. G., & Que, L., Jr. (1992) *Inorg. Chem.* *31*, 359–364.
- Ming, L.-J., Lynch, J. B., Holz, R. C., & Que, L., Jr. (1994) *Inorg. Chem.* *33*, 83–87.
- Neuhaus, D., & Williamson, M. P. (1989) in *The Nuclear Overhauser Effect in Structural and Conformational Analysis*, pp 30–38, VCH Publishing, Inc., New York.
- Oppenheimer, N. J., Rodriguez, L. O., & Hecht, S. M. (1979a) *Proc. Natl. Acad. Sci. U.S.A.* *76*, 5616–5620.
- Oppenheimer, N. J., Rodriguez, L. O., & Hecht, S. M. (1979b) *Biochemistry* *18*, 3439–3445.
- Oppenheimer, N. J., Rodriguez, L. O., & Hecht, S. M. (1980) *Biochemistry* *19*, 4096–4103.
- Oppenheimer, N. J., Chang, C., Chang, L. H., Ehrenfeld, G., Rodriguez, L. O., & Hecht, S. M. (1982) *J. Biol. Chem.* *257*, 1606–1609.
- Pillai, R. P., Lenkinski, R. E., Sakai, T. T., Geckle, J. M., Krishna, N. R., & Glickson, J. D. (1980) *Biochem. Biophys. Res. Commun.* *96*, 341–349.
- Scarrow, R. C., Pyrz, J. W., & Que, L., Jr. (1990) *J. Am. Chem. Soc.* *112*, 657–665.
- Spek, A. L., Duisenberg, A. J. M., & Feiters, M. C. (1983) *Acta Crystallogr. C* *39*, 1212–1218.
- Stubbe, J., & Kozarich, J. W. (1987) *Chem. Rev.* *87*, 1107–1136.
- Sugiura, Y. (1980) *J. Am. Chem. Soc.* *102*, 5216–5221.
- Takahashi, S., Sam, J. W., Peisach, J., & Rousseau, D. L. (1994) *J. Am. Chem. Soc.* *116*, 4408–4413.
- Takeshita, M., Grollman, A. P., Ohtsubo, E., & Ohtsubo, H. (1978) *Proc. Natl. Acad. Sci. U.S.A.* *75*, 5983–5987.
- Tan, J. D., Farinas, E. T., David, S. S., & Mascharak, P. K. (1994) *Inorg. Chem.* *33*, 4295–4308.
- Tolman, W. B., Shuncheng, L., Bentsen, J. G., & Lippard, S. J. (1991) *J. Am. Chem. Soc.* *113*, 152–164.
- Umezawa, H. (1973) *Biomedicine* *18*, 459–475.
- Vos, C. M., Westera, G., & Shipper, D. (1980) *J. Inorg. Biochem.* *13*, 165–169.
- Wang, Z., Ming, L.-J., Que, L., Jr., Vincent, J. B., Crowder, M. W., & Averill, B. A. (1992) *Biochemistry* *31*, 5263–5268.
- Wang, Z., Holman, T. R., & Que, L., Jr. (1993) *Magn. Reson. Chem.* *31*, 78–84.
- Westre, T. E., Loeb, K. E., Zaleski, J. M., Hedman, B., Hodgson, K. O., & Solomon, E. I. (1995) *J. Am. Chem. Soc.* *117*, 1309–1313.
- Williamson, D., McLennan, I. J., Bax, A., Gamcsik, M. P., & Glickson, J. D. (1990) *J. Biomol. Struct. Dyn.* *8*, 375–398.
- Wu, F.-J., & Kurtz, D. M., Jr. (1989) *J. Am. Chem. Soc.* *111*, 6563–6572.
- Wu, W., Vanderwall, D. E., Stubbe, J., Kozarich, J. W., & Turner, C. J. (1994) *J. Am. Chem. Soc.* *116*, 10843–10844.
- Wu, W., Vanderwall, D. E., Lui, S. M., Tang, X.-J., Turner, C. J., Kozarich, J. W., & Stubbe, J. (1996a) *J. Am. Chem. Soc.* *118*, 1268–1280.
- Wu, W., Vanderwall, D. E., Turner, C. J., Kozarich, J. W., & Stubbe, J. (1996b) *J. Am. Chem. Soc.* *118*, 1281–1294.
- Xu, R. X., Nettesheim, D., Otvos, J. D., & Petering, D. H. (1994) *Biochemistry* *33*, 907–916.
- Zang, Y., & Que, L., Jr. (1995) *Inorg. Chem.* *34*, 1030–1035.

BI962748T